Verification: Predicted Performance Output

The verification of the predicted performance output to the actual performance observed during the operation phase is the most difficult but most important verification step. In addition to the deviations of the as-built structure (probably minor) and of the selection of the design input variables (probably major), this verification analysis results in another deviation, i.e., the error introduced by the performance or design model itself. Thus, this verification should concern itself not only with structural performance, but also with functional criteria. In addition, it is possible that deviations in the design input variables will cancel each other out (e.g., a conservative estimate of strength could be balanced by an unconservative estimate of traffic).

The importance of obtaining a predicted-performance history similar to that observed is that it directly affects the economics, rehabilitation planning, existing load capacity, and remaining-life considerations.

SUGGESTED FRAMEWORK

A general conceptual framework for airport pavement evaluation is presented. The evaluation procedure should include surveys of (a) structural evaluation, (b) aircraft traffic, and (c) pavement conditions.

Each of these should be done at regular (periodic) intervals to obtain the optimum use of the data collection system. The structural-evaluation survey should have as its ultimate object the evaluation of layer and pavement response (i.e., strength, modulus, and deflection). The evaluation of the layer responses could be done at longer intervals, but at least the initial evaluation should use both destructive tests and field or laboratory tests. Deflection measurements (preferably dynamic) should be obtained at the same intervals as those recommended for the traffic and condition surveys.

The aircraft-traffic surveys can be made at any convenient time interval. Because this information is generally available from the airport administration, the major effort of this phase is the reduction of the information to a format that will be usable by the pavement engineer.

The condition surveys should be conducted at frequent intervals; the object of this operation should be to obtain information about the type and severity of visual pavement defects, the skid resistance of the pavement (runway), and either the profiling or measurement of the pavement roughness.

A general schematic illustrating these concepts is shown in Figure 5.

REFERENCES

1. Design Charts for Flexible Pavements. Shell International Petroleum Co., London, 1963.
2. J. H. Havens, R. C. Deen, and H. F. Southgate. Pavement Design Schema. HRB, Special Report 140, 1973, pp. 130-142.
3. R. C. Deen, H. F. Southgate, and J. H. Havens. Structural Analysis of Bituminous Concrete. HRB, Highway Research Record 407, 1972, pp. 22-35.
4. W. N. Brabston, W. R. Barker, and C. G. Harvey. Development of a Structural Design Procedure for All-Bituminous Concrete Pavements for Military Roads. USACE-WES, Technical Rept. S-75-10, Vicksburg, MS, July 1975.
5. Full-Depth Asphalt Pavements for Air Carrier Airports. Asphalt Institute, College Park, MD, Manual Series 11, Jan. 1973.
6. J. M. Edwards and C. P. Valkering. Structural Design of Asphalt Pavements for Heavy Aircraft. Koninklijke-Shell, Amsterdam, Construction Service Publication, 1971.
7. F. Finn, C. L. Saraf, and W. Smith. Development of Pavement Structural Subsystems. NCHRP, Project 1-10B; Final Rept., Materials Research and Development Corp., July 1976.
8. Federal Aviation Administration: New Pavement Design and Evaluation Methodology: Engineering and Development Plan. U.S. Army Engineer Waterways Experiment Station, Vicksburg, MS, Aug. 1975.
9. M. P. Jones. Analysis of the Subgrade Modulus and Pavement Fatigue on the San Diego Test Road. Univ. of Maryland, MSCE thesis, 1975.
10. M. W. Witczak. Full-Depth Asphalt Pavement for Dallas-Fort Worth Regional Airport. Asphalt Institute, College Park, MD, Res. Rept. 70-3, 1970.
11. M. W. Witczak. Prediction of Equivalent Damage Repetitions From Aircraft Traffic Mixtures for Full-Depth Asphalt Airfield Pavements. Proc., AAPT, Vol. 42, 1973, pp. 277-299.
12. M. W. Witczak. Development of a Full-Depth Design Procedure for Naval Air Stations. Naval Facilities Engineering Command, N00025-75-C-0002, 1976.
13. E. J. Yoder and M. W. Witczak. Principles of Pavement Design. Wiley, New York, 1975.

Aircraft Pavement Loading: Static and Dynamic

R. C. O'Massey, Douglas Aircraft Company, McDonnell Douglas Corporation, Long Beach, California

The subject of pavement loading by aircraft is treated by presenting a series of tables and figures designed to cover the essentials of pavement loading through the various phases of aircraft operation. The phases include static, slow taxi, steady-state turns at various speeds and turn radii, takeoff roll, roughness, landing impact, and braking. Figures and tables that present DC-8 responses at a number of international airports are also included.

This paper presents information of two kinds: The first is that concerning pavement loading such as is published in National Aircraft Standard 3601 documents (1, 2, 3) and widely disseminated by all major aircraft companies, and the second is an attempt to show by selected tables and charts the answers to a wide range of questions that have been discussed over the years.

Aircraft overall performance, strength, and performance of functional components (such as landing gear, tires, and brakes) are subject to federal regulation, which leads to a natural tendency to present information by using aeronautical terminology [e.g., the airplane

Figure 1. DC-9 series 30: %MAC versus station relations.

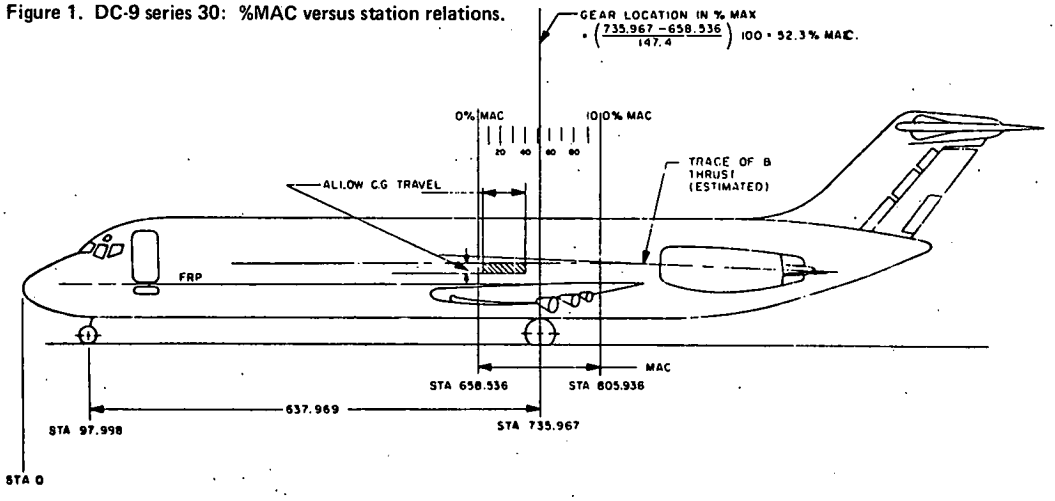

Table 1. Categorized summary of airport pavement loading.

Item	Title	Aircraft Operational Phase(s)	Purpose
Figure 1	%MAC versus station relations	All	To show envelope of aircraft center of gravity and mass (usually specified as %MAC)
Figure 2	Landing-gear loading on pavement	Static	To relate %MAC to percentage of mass to landing gear; to show Federal Aviation Administration certification center-of-gravity envelopes
Figure 3	Minimum turn radius versus taxi speed	Steady-state turns	To show centrifugal forces on turns and max g for passenger comfort and for landing gear and tire design limits
Figure 4	Takeoff of DC-10-40	Takeoff roll	To show time history as nose lifts off (computer run)
Figure 5	Gear configurations and centers of gravity	—	To locate loads given in Table 2
Table 2	Maximum pavement loads	Static and steady braking	To show max static pavement loading at main gear, max nose gear loading for steady braking, and max possible main gear drag loads
Table 3	Sources of vibration	All	To present data for passenger comfort considerations
Table 4	Aircraft operational phase and accompanying vibration sources	All	To present data for passenger comfort considerations
Table 5	Pavement unevenness for design, analysis, and evaluation	Taxiing, takeoff roll, landing roll, and rollout	To present data for passenger comfort considerations
Figure 6	Discrete 1 - cosine bump height versus wavelength	Takeoff and landing rolls	To present pavement bump criteria
Figure 7	Runway roughness for aircraft design	Takeoff and landing rolls	To present pavement bump criteria for aircraft design
Figure 8	Condition at touchdown	Touchdown	To show touchdown conditions at max design sink speed
Figure 9	Cross section of typical shock strut	—	To show mechanism of shock strut
Figure 10	Strut at half stroke; tire one-third deflected	—	To show airplane vertical displacement as function of strut stroke and tire deflection
Figure 11	Computerized landing program	—	To present structure of computerized landing program
Figure 12	Load versus stroke	Touchdown	To show load variation as a function of sink speed
Figure 13	Load versus time	Touchdown	To show strut load as a function of time from touchdown
Figure 14	Main landing-gear load	Landing impact	To show that landing-impact loads rarely exceed max static loads
Figure 15	Acceleration power spectra: DC-10-30/40	Takeoff	To show variation in acceleration power spectral density on smooth and rough pavements
Table 6	Landing-gear characteristics	Static at max takeoff load	To present required tire pressure, contact area, and wheel spacing of aircraft
Table 7	Airport pavement requirements	Static at max takeoff load	To present required airport pavement thicknesses

center of gravity as percentage of the mean aerodynamic chord (%MAC)]. This is because the envelope of the aircraft mass and center of gravity, which concerns the allowable limits for aerodynamic flight control, and the aerodynamic, flight-test, and certification data (e.g., legal limits) are all in terms of %MAC. Figure 1 presents the relation between %MAC and aircraft stationing, which is similar to civil engineering practice. Another aeronautical-industry communication problem, again arising from certification needs, is the wide distribution of maximum-critical cases that are necessary for aircraft safety, but obviously occur extremely rarely. However, for this reason, the paragraphs describing a number of the figures use the more typical day-in-and-day-out values of parameters.

Table 1 summarizes the figures and tables to orient the reader to the primary messages that they contain. The paper follows the organization of Table 1 with brief descriptive paragraphs as necessary to amplify the information given there.

BASIC AIRCRAFT DIMENSIONS

Figure 1 gives the information needed to relate the %MAC to the aircraft stations and dimensions [i.e., the stations corresponding to the leading edge and trailing edge and the length of the MAC [374.4 cm (147.4 in)]]. The MAC length may be different for different aircraft series; e.g., that of the DC-10-30/40 is different from that of the DC-10-10 because the former has a larger wing.

Figure 2. Landing gear loading on pavement: (a) DC-8-63, (b) DC-9-51, (c) DC-10-10, and (d) DC-10-30/40.

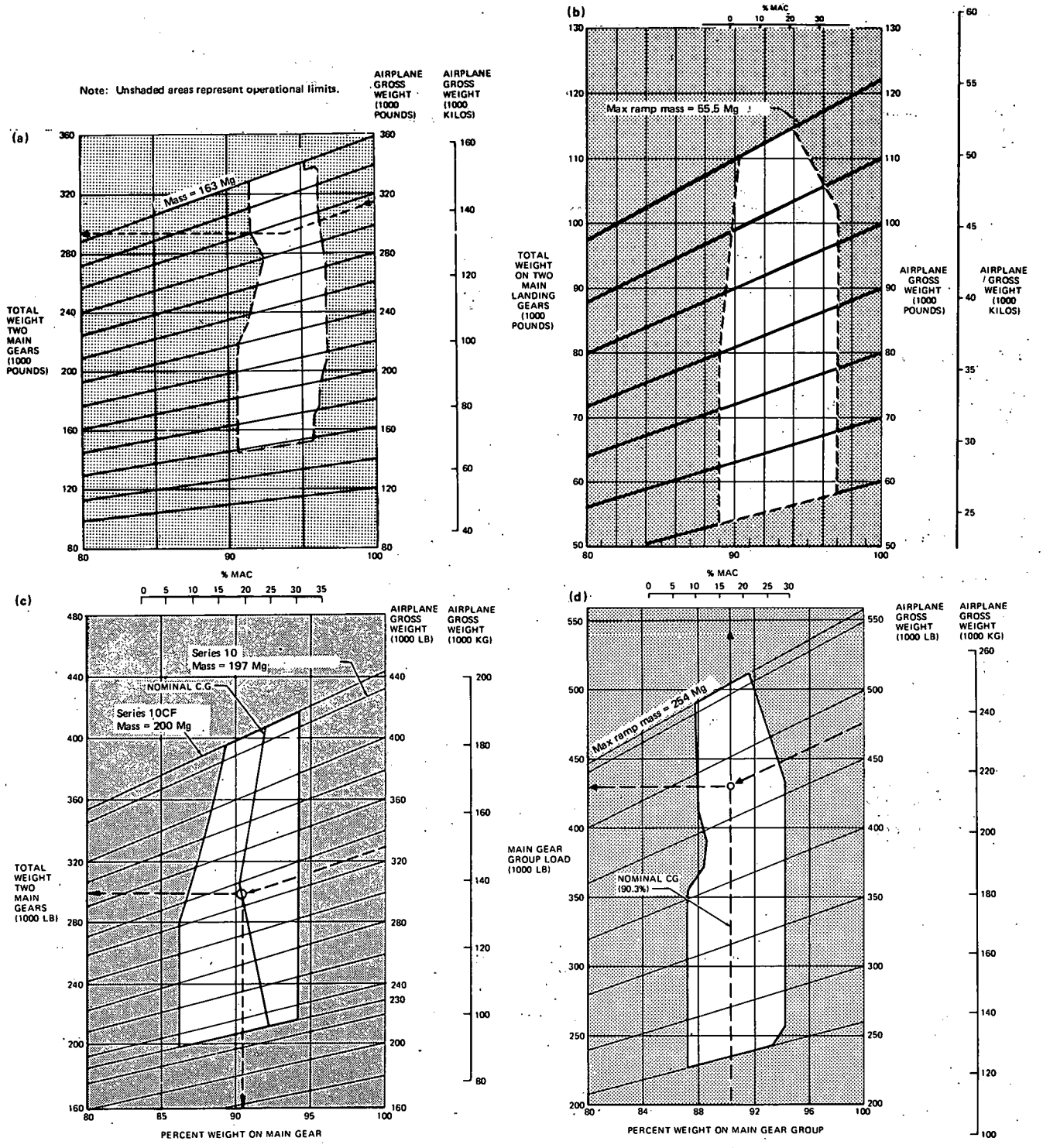

MASS AND CENTER-OF-GRAVITY ENVELOPES

Figure 2 (1, 2, 3) shows the allowable mass and center-of-gravity envelopes for the DC-8-63, DC-9-51, DC-10-10, series 10 and 10CF, and DC-10-30, 30CF, 40, and 40CF. Figure 2d also shows the nominal center of gravity variation with mass. Although the %MAC values vary greatly among airplanes, the percentage of the maximum gross mass to the landing gear for a nominal center of gravity varies less and is approximately 92 percent for a general average of contemporary jet aircraft.

STEADY TURNS

Figure 3 relates lateral accelerations to turn radii and speed and shows that 0.5 g is not only a landing-gear and tire design limit, but also requires friction coefficients exceeding 0.8 (very high). The 0.25 g curve represents a lateral maximum for passenger comfort.

Figure 3. Minimum turn radius versus taxi speed: DC-10.

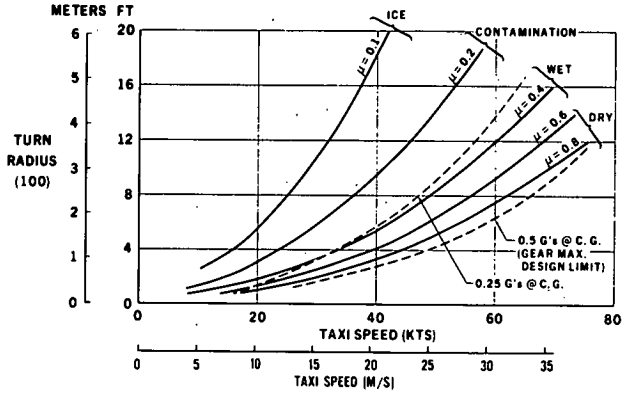

Figure 4. Takeoff of DC-10-40.

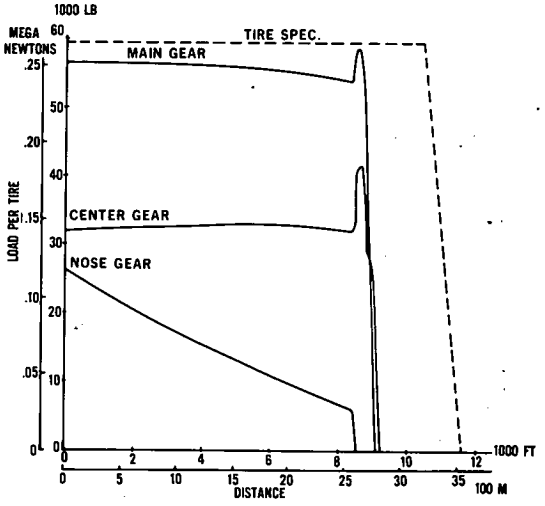

Notes: JT9D-59A engines.
Altitude = sea level; temperature = 25°C (77°F).
Elevator and time history
input: variable angle of attack, flat runway, and extremely hard rotation.
Dashed line shows tire test qualification.

Figure 5. Gear configurations and centers of gravity.

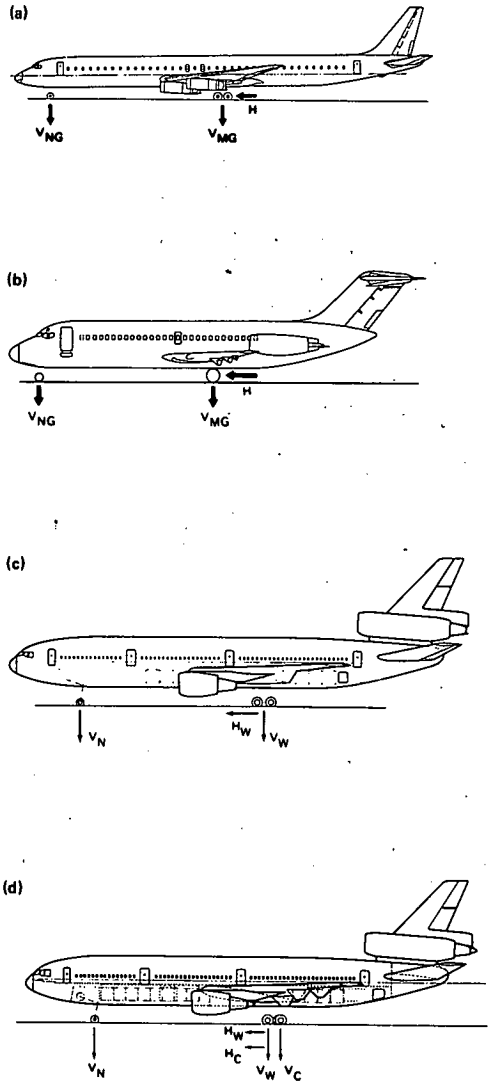

Table 2. Maximum pavement loads.

Model	Max Gross Mass (Mg)	Main Gear					Wing Gear			Center Gear		
		V_N or V_{NG} (kN)		V_{MG} per Strut (kN)		H per Strut (kN) (instantaneous braking)	V_W (kN)		H_W (kN) (instantaneous braking)	V_C (kN)		H_C (kN) (instantaneous braking)
		Static	Steady Braking	Static	Steady Braking		Static	Steady Braking		Static	Steady Braking	
DC-8												
-43	145	144.81	223.79	658.72	619.24	208.99	—	—	—	—	—	—
-55	149	151.40	232.87	690.39	650.04	219.15	—	—	—	—	—	—
-55F	149	161.90	243.38	691.12	650.25	219.22	—	—	—	—	—	—
-61	149	122.07	183.97	701.34	670.05	229.32	—	—	—	—	—	—
-61F	151	114.00	247.87	707.01	670.08	229.43	—	—	—	—	—	—
-62	154	156.72	323.52	733.24	692.42	234.68	—	—	—	—	—	—
-62F	154	160.82	327.14	746.89	706.07	226.68	—	—	—	—	—	—
-63	158	135.49	287.18	765.71	720.70	245.99	—	—	—	—	—	—
-63F	158	136.43	288.06	765.71	720.70	245.99	—	—	—	—	—	—
DC-9												
-15	41.6	39.356	69.905	18.805	175.58	129.36	—	—	—	—	—	—
-21	45.9	50.921	80.225	21.203	197.38	145.23	—	—	—	—	—	—
-32	49.5	51.072	77.043	22.410	211.12	157.52	—	—	—	—	—	—
-41	52.3	50.690	76.629	23.949	226.52	169.38	—	—	—	—	—	—
-51	55.5	52.390	73.643	25.500	244.38	185.32	—	—	—	—	—	—
DC-10												
-10	196	186.90	318.63	—	—	—	905.62	839.76	616.01	—	—	—
-10F	201	190.42	325.99	—	—	—	926.53	859.15	630.24	—	—	—
-30	253	307.90	217.00	—	—	—	936.87	866.80	636.86	405.74	375.41	275.82

Note: 1 Mg = 2200 lb and 1 kN = 224 lbf.

Table 3. Sources of vibration.

Source	Character	Frequency Range (Hz)	Most Significant Frequency (Hz)
Landing impact	Pulse	1 to 10	1 to 5
Runway roughness	Random	0.5 to 30	0.5 to 5
Atmospheric turbulence	Random	0 to 20	0 to 10
Buffet and oscillatory shocks	Random	1 to 50	1 to 20

Table 4. Aircraft operational phase and accompanying vibration sources.

Operational Phase	Approximate Time Duration (min)	Rough Runway	Jet Exhaust	Atmospheric Turbulence	Boundary-Layer Turbulence	Engine-Induced Buffet	Landing Impact
Warm-up	1 to 15	—	x	—	—	—	—
Taxi	5 to 15	x	x	—	—	—	—
Run-up	2 to 20	—	x	—	—	x	—
Takeoff	1 to 5	x	x	x	—	x	—
Climb	3 to 30	—	x	x	x	x	—
Cruise flight maneuver	60 to 480	—	x	x	x	x	—
Descent	5 to 15	—	—	x	x	x	—
Extend flaps and gear	1 to 15	—	—	x	—	x	—
Landing	0.08	x	—	—	—	x	x
Rollout	1 to 2	x	—	—	—	—	—

Figure 6. Discrete 1 - cosine bump height versus wavelength.

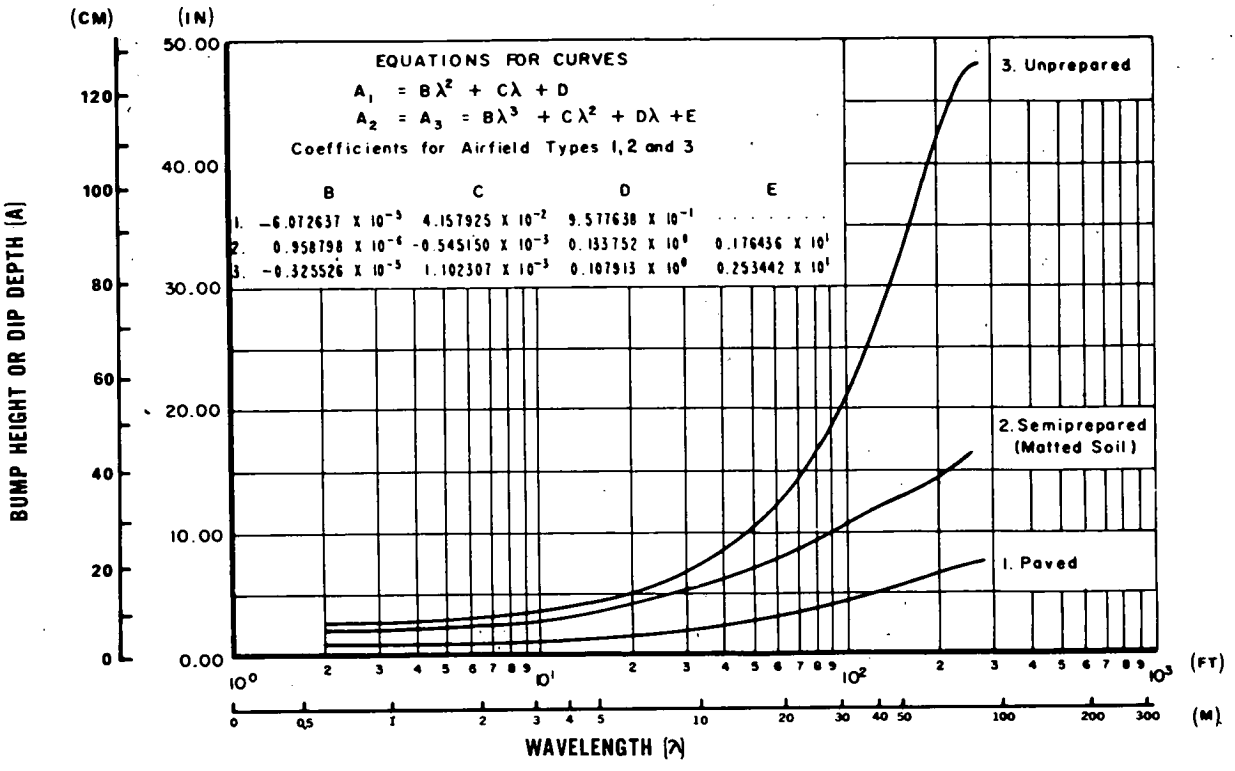

Figure 7. Runway roughness for aircraft design.

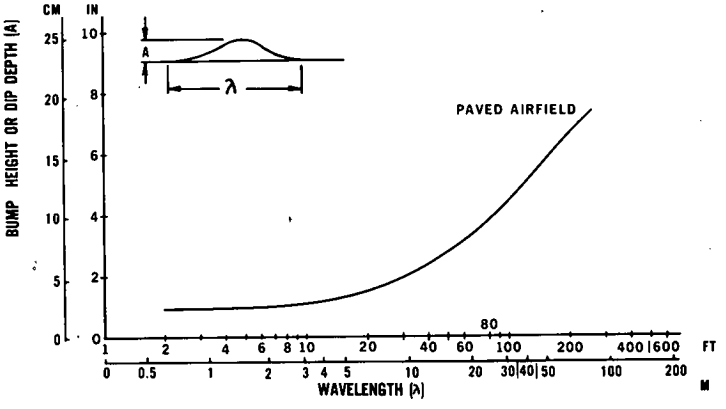

Table 5. Pavement unevenness for design, analysis, and evaluation.

Type of Unevenness	Estimated Percentage of Airports	No. or Duration	Dominant Response
Design grade runway over-crossings	100	2 to 5/flight	Rigid body modes
Slab faulting and spalling	5 to 10	—	Flexural modes; noise
Settling of slab centers	5 to 10	Length of runway or taxiway	Rigid body modes; flexural modes; noise
Washboarding	—	—	Rigid body modes; flexural modes; noise
Runway roughness spectra	50 to 70 to 90	—	Rigid and flexural modes; noise

Figure 8. Condition at touchdown.

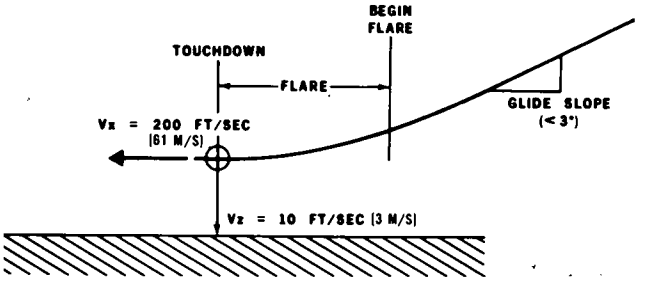

Note: Maximum landing force = 356 kN (80 000 lbf), 1.2 x V stall = Vx = 61 M/S (200 ft/s), and maximum design sink speed V_z = 3 M/S (10 ft/S).

Figure 9. Cross section of typical shock strut.

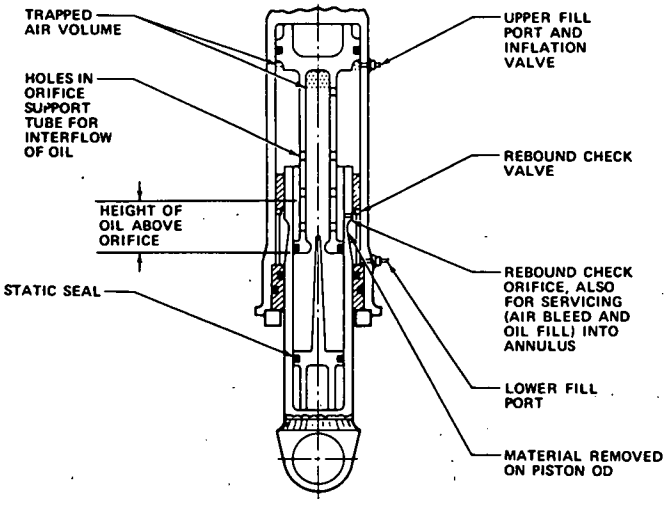

Figure 10. Strut at half stroke; tire one-third deflected.

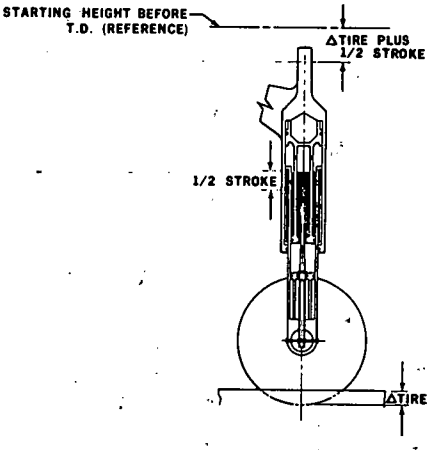

Figure 11. Computerized landing program.

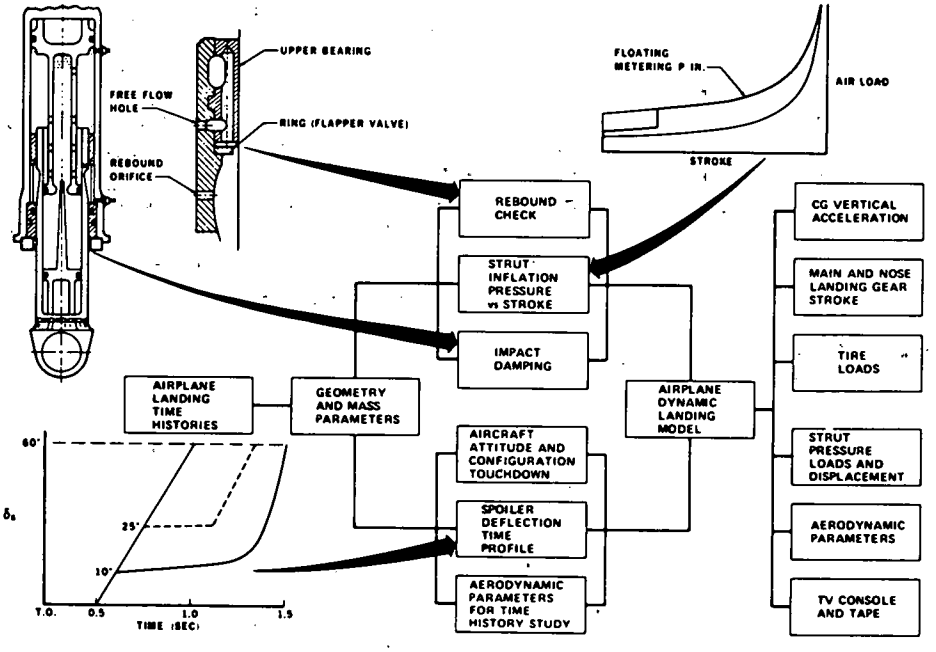

Figure 12. Load versus stroke.

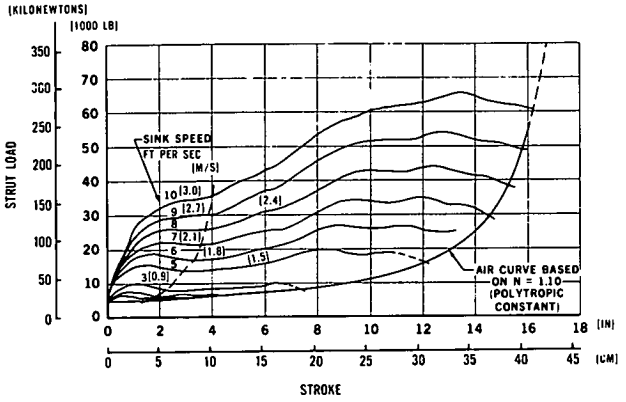

Figure 13. Load versus time.

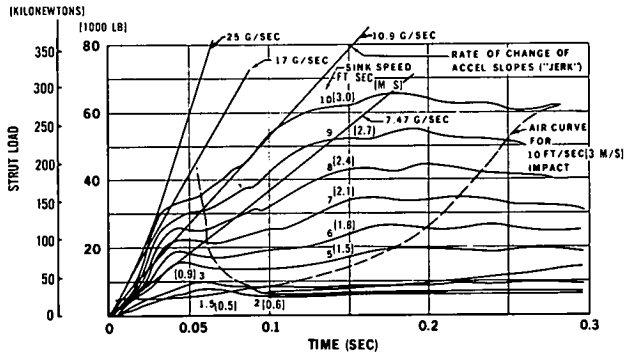

Figure 14. Main landing-gear load: DC-10-30/40 with (a) center gear extended and (b) center gear retracted.

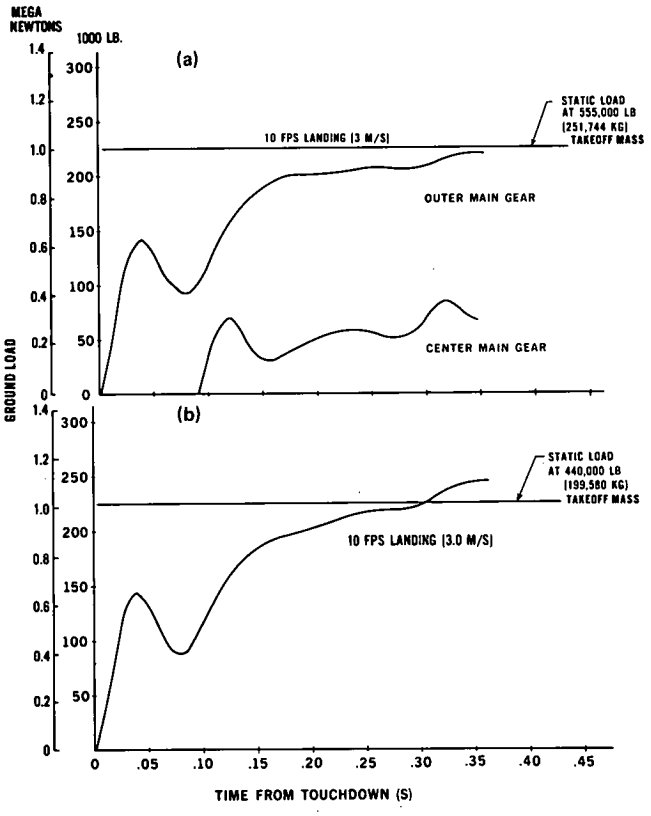

Figure 15. Acceleration power spectra: DC-8-63 at (a) cockpit, (b) center of gravity, and (c) pylon no. 3.

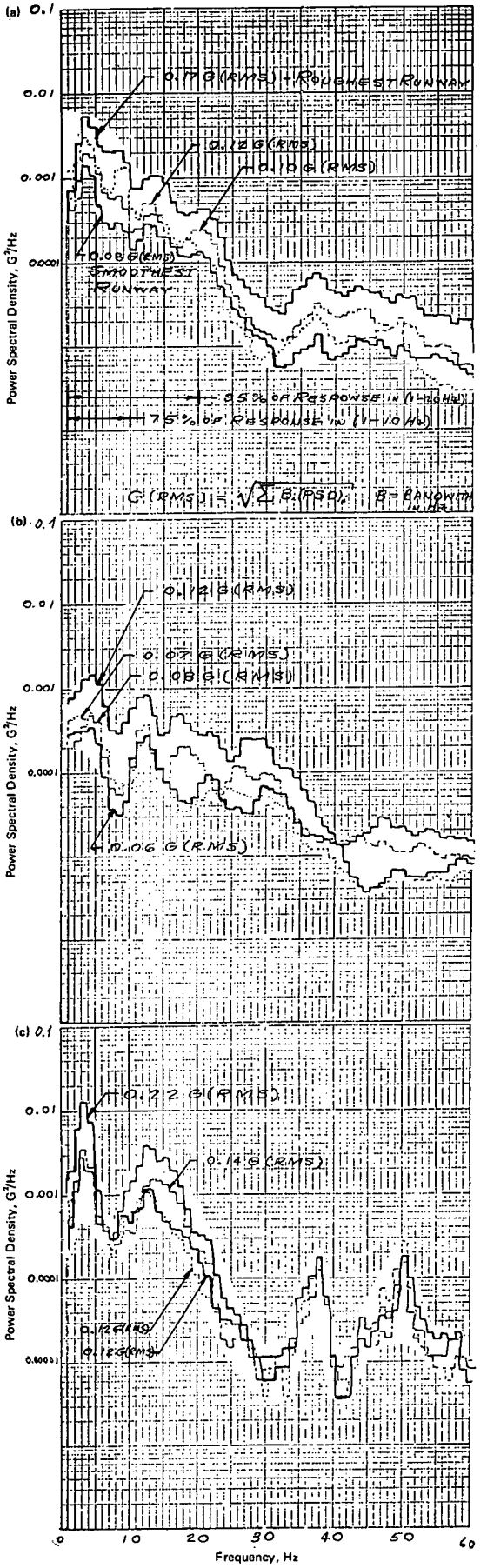

Table 6. Landing-gear characteristics.

Characteristic	DC-9-41	B-727-200	B-707-320	DC-8-55	DC-8-63	DC-10-10	DC-10-20/30	B-747	B-747B
Mass									
Max ramp, kg	52 163	78 472	152 407	148 779	162 386	200 942	253 105	323 412	352 895
Max takeoff, kg	51 710	78 018	151 934	147 418	161 026	199 581	251 744	322 051	351 535
Max landing, kg	42 266	72 575	112 037	98 430	124 738	157 397	182 798	255 826	255 826
Landing gear configuration	00	00	00	00	00	00	00	00	00
	00 00	00 00	00 00 00 00	00 00 00 00	00 00 00 00	00 00 00 00	00 00 00 00	00 00 00 00 00 00 00 00	00 00 00 00 00 00 00 00
Wing landing gear									
Tire size, mm	1041 by 381	1245 by 432	1168 by 406	1118 by 406	1130 by 419	1270 by 508	1321 by 521	1168 by 406	1245 by 432
Tire contact area, cm^2	1097	1529	1355	1348	1419	1781	2065	1355	1529
Tire pressure, kPa	114	116	124	130	134	121	114	141	128
Twin spacing, cm	66.0	86.4	87.9	76.2	81.3	137.2	137.2	111.8	111.8
Tandem spacing, cm	—	—	142.2	139.7	139.7	162.6	162.6	147.3	147.3
Center landing gear									
Tire size, mm	—	—	—	—	—	—	1321 by 521	—	—
Tire contact area, cm^2	—	—	—	—	—	—	2065	—	—
Tire pressure, kPa	—	—	—	—	—	—	97	—	—
Twin spacing, cm	—	—	—	—	—	—	95.3	—	—

Note: 1 kg = 2.2 lb, 1 mm = 0.039 in, 1 cm^2 = 0.155 in^2, and 1 kPa = 0.145 lbf/in^2.

Table 7. Airport pavement requirements at maximum takeoff mass.

Procedure	DC-9-41	B-727-200	B-707-320	DC-8-55	DC-8-63	DC-10-10	DC-10-20/30	B-747	B-747B
Airplane load classification number (LCN)									
Rigid pavement									
L = 75 cm	59	78	70	74	80	73	73	73	74
L = 100 cm	61	81	82	86	92	84	84	85	86
L = 125 cm	62	84	91	94	102	94	94	94	96
Flexible pavement									
H = 50 cm	56	72	79	85	90	74	75	77	79
H = 75 cm	63	81	94	100	107	91	91	94	96
H = 100 cm	68	88	106	112	120	105	105	107	109
Pavement thickness (cm)									
Concrete[a]	25.9	29.0	31.2	31.8	32.3	31.5	31.8	30.5	31.8
Flexible									
CBR = 10	53.3	64.0	77.0	77.7	81.8	81.8	83.8	75.7	81.0
CBR = 15	39.4	48.3	56.1	57.4	60.7	60.5	60.5	55.1	58.4

Note: 1 cm = 0.39 in.

[a] σ = 275 Pa and k = 80 Pa/cm.

TAKEOFF

Figure 4 depicts an unusual computer-study takeoff of a DC-10-40 aircraft in which the aircraft rotation for lift-off is so severe that the tail strikes the ground. It is included here to show the amount of peaking that can occur under extreme conditions. However, the rotation-bump magnitude was less than 10 percent above the load without a bump.

MAXIMUM PAVEMENT LOADING

Figure 5 shows the gear configurations and centers of gravity of the DC-8, DC-9, and DC-10 aircraft, and Table 2 shows their maximum pavement loads at a steady deceleration (braking) of 3.05 m/s^2 (10 ft/s^2) and an instantaneous braking coefficient of friction of 0.8. [These conditions are close to the aircraft maximum deceleration and the brake and tire design specifications; more typical day-in-and-day-out values are 1.8 m/s^2 (6 ft/s^2) and 0.35.]

The following notation is used:

$V_{NG} = V_N$ = max vertical nose-gear ground load at most forward center of gravity,
V_{MG} = max vertical main-gear ground load at most aft center of gravity,
H = max horizontal ground load from braking,
V_W = max vertical wing-gear ground load per strut at most aft center of gravity,
V_C = max vertical center-gear ground load per strut from braking,
H_W = max horizontal wing-gear ground load per strut from braking, and
H_C = max horizontal center-gear ground load per strut from braking

All loads are calculated by using max aircraft ramp force.

PASSENGER-COMFORT CONSIDERATIONS

Tables 3, 4, and 5 give general information about important vibration sources, exposure-time durations, frequencies of interest, and categories of pavement unevenness that are considered in aircraft design, usually

for passenger comfort rather than for aircraft-fatigue loading for which the ground-air-ground cycles of loading are more demanding.

PAVEMENT-BUMP CRITERIA

Figures 8 and 9 (4) show the discrete 1 - cosine bump heights that are used to define loads for the structural design of aircraft. Bump heights exceeding these criteria [e.g., 11.4 cm (4.5 in) in 30.5 m (100 ft)] may exceed the aircraft design loads. Special studies (which are expensive) are required to depart from these criteria, but have been done for special cases (e.g., to define allowable overlay tapers).

COMPUTER LANDING STUDY

The sequence of Figures 8 through 13 shows the inputs and results of a computer landing study. Figure 8 shows touchdown conditions at the maximum design sink speed of 3.05 m/s (10 ft/s) at the maximum landing force of 356 kN (80 000 lbf) and a horizontal speed of 1.2 times the airplane stall speed. Because the aircraft has flying speed, a lift equal to the landing force is acting throughout the landing impact so that the landing gear absorbs only the vertical kinetic energy.

Figure 9 shows that in the struts, the trapped oil is forced through an orifice whose annulus area is varied by a metering pin as a function of the stroke. This produces a reaction proportional to the strut stroking (collapsing) velocity squared and the amount of stroke. Figure 10 shows that the aircraft vertical displacement is a function of the strut stroke plus the tire deflection.

Figure 11 shows a block diagram chart of the inputs and outputs of the computerized landing-dynamics program. In this program, the engineer can work interactively with the computer via a cathode-ray-tube console.

Figure 12 shows the load variation as a function of aircraft sink speed at touchdown. In this figure, the impact is ended (i.e., the aircraft sink speed equals zero) when the load line crosses the air curve. For a typical airline landing [at a sink speed of approximately 1 m/s (3 ft/s)], the peak load is a fraction of the design sink-speed load and less than half the available stroke is used.

Figure 13 shows the strut load as a function of time. The impact time duration varies from 0.1 to less than 0.3 s.

Figure 14 shows comparisons between the maximum landing loads and the maximum static takeoff loading. For the landing with the centerline gear extended, the maximum landing load is less than the static takeoff load. For the landing with the centerline gear retracted, the load is less than 10 percent above the static takeoff load.

RUNWAY ROUGHNESS RESPONSE AT FOUR INTERNATIONAL AIRFIELDS

Figure 15 shows the acceleration response of the DC-8-63 aircraft at four international airports. Power spectral density as a function of frequency was measured at (a) the cockpit floor, (b) the aircraft center of gravity, and (c) engine pylon no. 3. The upper solid lines show the responses at the roughest airport, and the lower solid lines show the responses at the smoothest airport. Root-mean-square values for each of the curves provide a clear response index from rough to smooth. The primary message contained in these data is based on the following heuristic discussion.

1. The study was conducted to identify a pavement roughness problem at a particular airport that pilots had complained about for three years because of a number of engine acceleration warning light occurrences on takeoff.
2. Except for minor local landing-gear failures that had been repaired by parts replacement, there was no structural fatigue damage attributable to the rough runway operation.

Therefore, a highly objectionable ride due to runway roughness is tolerated by the aircraft without incurring fatigue damage. This statement is not an endorsement for rough runways; it only places the problem in perspective. Rough runways are still highly objectionable because they damage aircraft instruments and sensitive electronic equipment and disturb pilot and passenger sense of safety.

COMPARATIVE LANDING-GEAR AND AIRPORT CHARACTERISTICS

Table 6 gives typical, frequently requested data about aircraft loading and landing-gear characteristics, and Table 7 gives pavement requirements by international (5) and United States procedures (i.e., the Portland Cement Association PDILB computer program for concrete thicknesses and the U.S. Air Force SEFL 16SA program for flexible pavement thicknesses). The data are based on takeoff mass and assume a constant distribution of the mass of 92 percent to the main landing gear.

ACKNOWLEDGMENT

I wish to thank the Scandinavian Airlines System (SAS) for permission to use the data contained in Figure 15 and acknowledge the assistance of Ole Riis-Hansen and Sig Jonasson of SAS and Edmond Zwiback of Douglas Aircraft Company. It was a pleasure to work with them on a program with such excellent instrumentation, recording, and processing of the data.

REFERENCES

1. DC-8 Airplane Characteristics: Airport Planning. Douglas Aircraft Company, Rept. 67492, March 1969.
2. DC-9 Airplane Characteristics: Airport Planning. Douglas Aircraft Company, Rept. 67264, June 1975.
3. DC-10 Airplane Characteristics: Airport Planning. Douglas Aircraft Company, Rept. 67803, Nov. 1973.
4. Airplane Strength and Rigidity, Landing, and Ground-Handling Loads. U.S. Air Force, Military Specification MIL-A-008862A, March 31, 1971.
5. Aerodrome Manual, International Civil Aviation Organization, 1965.